A PHYSICS-BASED DESCRIPTION OF INTER-GRANULAR HELIUM BEHAVIOUR IN SCIANTIX FOR APPLICATION IN FUEL PERFORMANCE CODES

R. GIORGI, A. CECHET, L. COGNINI, A. MAGNI, D. PIZZOCRI, L. LUZZI

Politecnico di Milano, Department of Energy, Nuclear Engineering Division, via La Masa 34, 20156 Milano - Italy

A. SCHUBERT, P. VAN UFFELEN

European Commission, Joint Research Centre, Directorate for Nuclear Safety and Security, P.O. Box 2340, 76125 Karlsruhe - Germany

ABSTRACT

In this work, we propose a new mechanistic model for the treatment of helium behaviour at grain boundaries in oxide nuclear fuel. The model pairs rate-theory description of helium intra-granular behaviour (diffusion towards grain boundaries, trapping in spherical bubbles, thermal re-solution), developed in a first step, with rate-theory description of helium inter-granular behaviour (diffusion towards grain edges, trapping in lenticular bubbles, thermal re-solution). The proposed model has been implemented in SCIANTIX (meso-scale software designed for coupling with fuel performance codes) and validated against thermal desorption experiments performed on doped UO_2 samples annealed at different temperatures. The overall agreement of the new model with the experimental data is satisfactory, both in terms of integral helium release and of helium release rate, showing an improvement compared to previous mechanistic models, which do not consider the behaviour of helium at grain boundaries. By considering the contribution of helium at grain boundaries it is possible to represent the kinetics of helium release rate at high temperature. Given the uncertainties involved in the initial conditions for the inter-granular part of the model (initial helium concentrations in inter-granular bubbles, and in solution at grain boundaries) and the uncertainties associated to some model parameters for which limited lower-length scale information is available (helium diffusivity at the grain boundaries in particular) the results are complemented by a dedicated sensitivity analysis. This analysis demonstrates that the initial conditions, if chosen in a reasonable range, have limited impact on the results, and confirms that it is possible to achieve satisfying validation results using sound values for the uncertain physical parameters.

1. Introduction

The description of helium behaviour in nuclear fuel is of engineering interest, both in irradiation conditions, since, together with xenon and krypton, it concurs to the gaseous swelling of the fuel pin and gas release in the free volume of the fuel rod, and in storage (since it is produced in large amount due to the α-decay of actinides). Currently, in the state-of-the-art models[1]–[6] used in thermo-mechanical fuel performance codes [7]–[9], the description of gas and helium behaviour is approached in three sequential steps [10], [11]: first production, then intra-granular evolution [12]–[15] and lastly inter-granular evolution [16]. The rate-theory model proposed in this work is similarly designed and is intended for application in fuel performance codes, extending the capabilities of currently available models [10]. The focus is on including the physical description of inter-granular helium behaviour to improve the predicting capabilities of helium evolution in annealing conditions i.e., to be able to reproduce both the peaks (also that at lower temperature, besides the higher temperature one) of the helium release rate (see [10] for the results from the intra-granular helium model alone). The model has been implemented in SCIANTIX [17] (meso-scale software designed for coupling with fuel performance codes). Given the uncertainties involved in the initial conditions for the inter-granular part of the model (i.e., the initial helium concentration in inter-granular bubbles, and in solution at grain boundaries) and the uncertainties associated to some model parameters for which limited lower-length scale information is available (helium diffusivity at the grain boundaries in particular) the results are complemented by a dedicated sensitivity analysis. The description of the model is performed in Section 2, including an introduction to the various parameter involved (Table 1). The results obtained are showcased and described in Section 3, while the outcomes of the sensitivity analyses on initial conditions and physical model parameters are reported in Section 4.

2. Model Description

We herein outline the equations governing the evolution of the in-bubble and single-atom helium concentrations at grain boundaries

$$\frac{\partial c_{gb}}{\partial t} = S(1-F) + D_{gb}\nabla^2 c_{gb} - g_{gb}\left(c_{gb} - c_{s,gb}\right) + b_{gb}m_{gb} - \nu_{gb}n_{gb}$$
$$\frac{\partial m_{gb}}{\partial t} = SF + g_{gb}\left(c_{gb} - c_{s,gb}\right) - b_{gb}m_{gb} + \nu_{gb}n_{gb} \quad (1)$$

where *S* (at m^{-2} s^{-1}) represents the helium source coming from within the grain, D_{gb} (m^2 s^{-1}) is the inter-granular helium diffusion coefficient, c_{gb} (at m^{-2}) is the inter-granular single atom helium concentration, $c_{s,gb}$ (at m^{-2}) is the solubility of helium at grain boundaries, g_{gb} (s^{-1}) is the trapping rate, b_{gb} (s^{-1}) is the irradiation induced re-solution term, m_{gb} (at m^{-2}) is the helium concentration in inter-granular bubbles, ν_{gb} (bub s^{-1}) is the nucleation term, n_{gb} ($\mathrm{at\,bub^{-1}}$) is the number of helium atoms per inter-granular bubble and *F* (/) is the fractional coverage of grain faces, which acts as a parameter that distributes (distribution factor) helium reaching the boundary between inter-granular bubbles and solution.

Some considerations are made to develop Eq. 1. We assumed that at the boundary helium moves on a 2D space, thus diffusion will act accordingly. The spherical Laplacian becomes cylindrical with the only relevant portion of it being the radial one:

$$D_{gb}\nabla^2 c_{gb} = D_{gb}\frac{1}{r}\frac{\partial}{\partial r} r \frac{\partial}{\partial r} c_{gb} \quad (2)$$

As far as the source term is concerned, we said that the source of grain boundary helium comes from within the grain itself. Diffusion of intra-granular helium towards the boundary is what represents our inter-granular source. This makes the grain boundary evolution dependent on the intra-granular behaviour.

For *S* to be expressed coherently, the intra-granular helium single atom concentration c_{ig} ($\mathrm{at\,m^{-3}}$) needs to be rescaled on a 2D space by means of the surface to volume ratio of the spherical grain radius which is equal to one third of the spherical grain radius itself, i.e., $c_{ig,gb} = \frac{a}{3}c_{ig}$, where $c_{ig,gb}$ (at m^{-2}) is the contribution to grain boundary helium coming from within the grain and a (m) is the spherical grain. Thus, the expression of S (which corresponds to the intra-granular concentration diffusing out of the spherical grain and entering a cylindrical grain face, coupling intra- and inter-granular behaviour) becomes:

$$S = -\frac{a}{3}D_{ig}\frac{1}{r_*^2}\frac{\partial}{\partial r_*} r_*^2 \frac{\partial}{\partial r} c_{ig} \quad (3)$$

where D_{ig} is the intra-granular diffusion coefficient (m^2 s^{-1}). The Laplacian of the source remains expressed in spherical coordinates because the diffusion which produces S takes place in the intra-granular framework.

In analogy with the intra-granular model [10], we included the helium solubility at grain boundaries that follows Henry's law, $c_{s,gb} = \frac{a}{3} k_H p_{gb}$, where k_H is the Henry constant [18], p_{gb} is the helium pressure at grain boundaries and $\frac{a}{3}$ is the surface to volume ratio (used as conversion factor). The solubility leads to a thermally activated re-solution of helium single atoms from bubbles in the form:

$$\gamma_{gb} m_{gb} = g_{gb} c_{s,gb} \tag{4}$$

where γ_{gb} (s^{-1}) is the inter-granular thermal re-solution rate.

In annealing conditions, the irradiation induced re-solution rate is null, $b_{gb} = 0$, and it is assumed that a bubble population is formed at the first time-step and then it evolves along the experiment [10], [19]; thus, if we substitute Eqs. 2, 3 and 4 into Eq. 1, the inter-granular equations become:

$$\begin{aligned} \frac{\partial c_{gb}}{\partial t} &= -\frac{a}{3} D_{ig} \frac{1}{r_*^2} \frac{\partial}{\partial r_*} r_*^2 \frac{\partial}{\partial r} c_{ig} (1 - F) + D_{gb} \frac{1}{r} \frac{\partial}{\partial r} r \frac{\partial}{\partial r} c_{gb} - g_{gb} c_{gb} \\ &\quad + \gamma_{gb} m_{gb} \\ \frac{\partial m_{gb}}{\partial t} &= -\frac{a}{3} D_{ig} \frac{1}{r_*^2} \frac{\partial}{\partial r_*} r_*^2 \frac{\partial}{\partial r} c_{ig} F + g_{gb} c_{gb} - \gamma_{gb} m_{gb} \end{aligned} \tag{5}$$

These equations are then coupled with those defining the model for the intra-granular helium evolution [10]. The various parameters involved in the inter-granular model can be found in **Table 1**.

Symbol	Description	Formula	units	Reference
$\boldsymbol{D_{ig}}$	Intra-granular diffusion coefficient	$2.0 \cdot 10^{-10} \exp(-2.12/kT)$	$\mathrm{m^2 s^{-1}}$	[10],[20]
$\boldsymbol{D_{gb}}$	Inter-granular diffusion coefficient	$10^3 \cdot D_{ig}$	$\mathrm{m^2 s^{-1}}$	Present work
$\boldsymbol{g_{gb}}$	Inter-granular trapping rate	$2\pi D_{gb} N_{gb} / \ln\left(1/R_{gb}\sqrt{\pi N_{gb}}\right)$	$\mathrm{s^{-1}}$	Present work,[21]
$\boldsymbol{c_{s,gb}}$	Inter-granular helium solubility	$\frac{a}{3} k_H p_{gb}$	$\mathrm{at\ m^{-2}}$	[10], [22 – 24]
$\boldsymbol{k_H}$	Henry's constant	$4.1 \cdot 10^{24} \exp(-0.65/kT)$	$\mathrm{at\ m^{-3} MPa^{-1}}$	[10], [18]
$\boldsymbol{\gamma_{gb}}$	Inter-granular thermal re-solution	$\frac{2\pi D_{gb}}{\ln\left(1/R_{gb}\sqrt{\pi N_{gb}}\right)} \frac{a}{3} k_H \frac{kT}{V_{gb}} Z$	$\mathrm{s^{-1}}$	Present work
$\boldsymbol{p_{gb}}$	Inter-granular helium bubble pressure	$kTZn_{gb}/V_{gb}$	Pa	
$\boldsymbol{F}$	Fractional coverage	$N_{gb} A_{gf}$	/	[16]
$\boldsymbol{V_{gb}}$	Average inter-granular bubble volume	$4\phi(\theta)\pi R_{gb}^3 / (3 sin^3(\theta))$	$\mathrm{m^3}$	[16]
$\boldsymbol{\phi(\theta)}$	Semi-dihedral factor of a bubble	$1 - 1.5\cos(\theta) + 0.5 cos^3(\theta)$	/	[16],[25]

Table 1: Parameters involved in the inter-granular model proposed in this work.

3. Results

For validation purposes, we tested the predictive capabilities of the model against a set of data on helium release and release rate collected by Talip et al. [19] during annealing measurements. The experiment was performed on UO_2 samples doped with 0.1 wt.% of additive containing 66.7 wt.% of $^{238}PuO_2$, whose α-decay produced helium atoms within the sample during an aging period of 15 years in a glovebox with inert atmosphere (N_2). The samples were than annealed in a Knudsen Effusion Mass Spectrometer and helium release was measured using a Quantitative Gas Measurement System (Q-GAMES) [26]. For the sake of brevity we decided to present only the results obtained for one of the temperature histories available [19]. In particular, the profile considered in this work is shown in **Figure 1**. We focused on the 1800 K irradiation history to show the improvement in predicting the double helium release peak brought about by the coupled intra- and inter-granular description with respect to the result from the intra-granular model alone, reported in [10].

The temperature history is characterised by a heat up ramp of 30 minutes at 10-20 K min^{-1} with a subsequent hold of the temperature, at a value of 1800 K, for 1-3 h. After the plateau, the temperature is decreased to 800 K.

We choose to present the results obtained at 1800 K because, in this annealing history, the improvement provided by the novel inter-granular model in predicting the helium release behaviour is mostly appreciable.

For the history considered, the behaviour of helium fractional release and helium release rate is reported. The results of the model incorporating the contribution of the grain boundaries are also compared to the previous version of the model (only intra-granular contribution) and with the aforementioned experimental results [19]. Modelling assumptions, necessary for the set-up of the SCIANTIX simulation are made on the inter-granular helium diffusion coefficient and on the fraction of helium initially considered at grain boundaries. In particular a reference value of 10% of the helium produced is taken for the fraction of helium initially present at boundary and the ratio D_{gb}/D_{ig} is assumed to be 10^3 [27].

Figure 2 shows that the inclusion of a model treating helium behaviour at grain boundaries provides a further step to enlighten the physical behaviour of this gas inside nuclear fuel. The helium release at 1800 K is improved but still slightly underestimated. This could be due to the uncertainty on the initial values of helium at the boundary (as explained in the following section). Also, the residual underestimation during the annealing at constant temperature calls for further extensions of the intra-granular helium model capabilities, controlling the release at this stage. As far as the helium release rate is concerned, the most noticeable remark is the double peak in the release rate of the 1800 K profile, as shown by the measured profile [19]. The presence of a peak at lower temperature, followed by a second one at higher temperature, is coherent with the fact that, as stated by Martin et al.[28], [29], the release of helium occurs in two successive stages. The first stage corresponds to the release of helium which is located a few microns either side of grain boundaries, where faster helium diffusion occurs (i.e., regions with higher diffusion rate). This is also consistent with the slightly lower activation energy for grain boundary diffusion obtained by Garcia et al. [27] and shown in **Figure 4** below, although the uncertainty on the activation energy is large. The second stage of helium release should occur via the slow re-solution and release of gas atoms trapped within grains.
Thus, helium at grain boundaries plays a relevant role on the overall helium behaviour and the evidence that the proposed model can correctly predict the two stages in which release occurs, is a promising achievement.

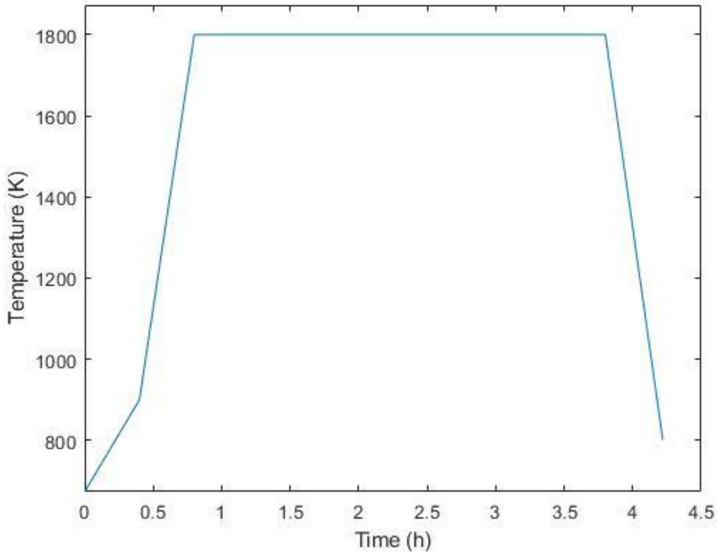

Figure 1: Temperature history of the annealing experiment [19] at 1800 K herein considered.

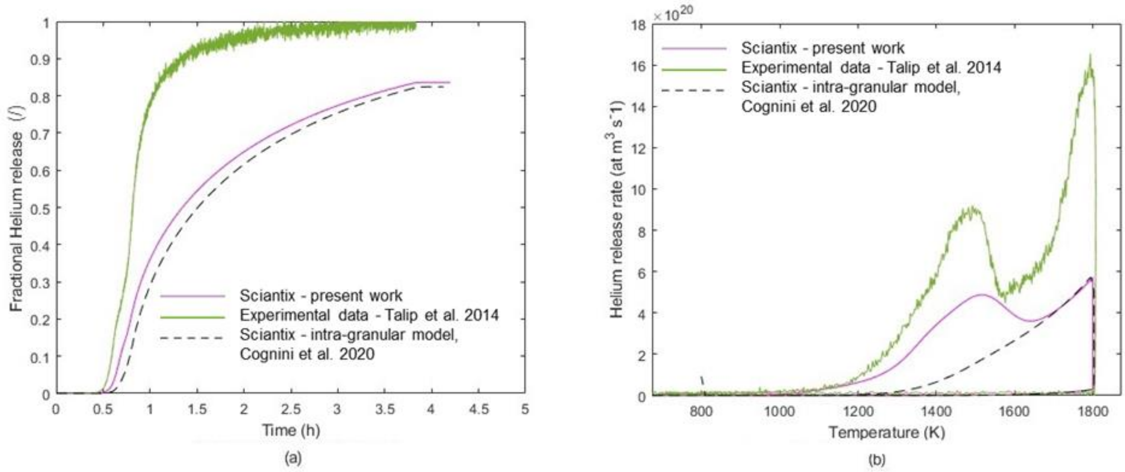

Figure 2: Comparison of SCIANTIX fractional helium release (a) and helium release rate (b) with experimental data provided by Talip et al.[19] from the temperature history at 1800K. The black dashed line represents the results from Cognini et al.[10] and the purple line the present development including grain boundary treatment.

4. Sensitivity analyses: parametric studies

Given the lack of experimental information on helium at grain boundaries, some assumptions were made on the initial values of some parameters of the model, namely the initial fraction of helium stored at the grain boundaries at the beginning of the annealing test and its distribution among inter-granular bubbles and inter-granular solution, together with the diffusivity of helium at the grain boundaries.

The hypothesis of considering an initial portion of the helium produced in the samples at grain boundaries comes from Martin et al. [28],who stated that a fraction of the helium initially produced in a sample is close enough to the boundaries to be considered at grain boundaries. As for the exact value for this initial boundary contribution, no experimental data are available. To throw light into this fundamental model parameter, mandatory for the initialization of the SCIANTIX simulation, a sensitivity analysis was performed, and a 10% fraction of the helium produced emerged as a value showing promising results (as can be seen from **Figure 2**). This value was then compared to others within an uncertainty range. The two extreme values of the interval chosen are 0%, that comes from the original model by Cognini et al**.** [10] which neglects the treatment of helium at grain boundary, and 20%, which emerged during the sensitivity analysis as the value beyond which the model started overestimating all the release rate peaks attributable to the helium at boundaries contribution. It is possible to see from **Figure 3(a)** that, within the chosen range of uncertainty, the effect on the overall release is a variation of around 3.5%, or a $\pm$1.75% with respect to the reference value (10%) of helium initially assumed to be at boundary.

Concerning how helium at grain boundaries is initially split between inter-granular solution and inter-granular bubbles, it is relevant to see how this subdivision could impact the fractional release and the release rate. To understand the influence of the aforementioned division, once again the behaviour determined by the annealing history at 1800 K is considered. Since no assessed data are available, this case also required a proper sensitivity analysis. The fraction of helium in bubbles was made to vary in a range between 0% to 50% of the total helium initially present at grain boundaries. **Figure 3(c)** and **Figure 3(d)** show that the initial helium distribution bears little to no effect on the overall fractional release, but it induces some changes on the first peak in helium release rate. This is reasonably within expectations, since how helium is distributed between bubbles and solution does not affect how much helium will ultimately be released (the integral of the release is not affected), while, on the other hand, having more helium in bubbles at the initial stages of release means that more gas needs to return in solution before release, slightly reducing the rate and vice versa (The derivative of the release is what perceives the effect of the split). This effect is then reflected on the first peak because it is the one associated to the release of helium initially present at grain boundaries (as already stated in Section 3). Nevertheless, we can see that even along a 50% range of uncertainty the effect of this parameter is relatively small. Future data collection on this open issue could provide a more detailed insight on how this initial split should be treated.

As far as the diffusion coefficient is concerned, the lack of experimental data for this specific case and, in general, for the definition of a specific coefficient, led to the choice of considering the same diffusion correlation adopted by Cognini et al.[10] in the intra-granular only version of this model, but increased by a certain factor defined by the ratio D_{gb}/D_{ig} (hence, keeping the same slope of the correlation in [10], coming from [20]).

Interesting results obtained by Garcia et al. [27] are presented in **Figure 4**, that shows values at different temperatures of the helium intra-granular and inter-granular diffusion coefficients in $\mathrm{UO_2}$ polycrystalline samples. The experimental scatter and the scarcity of data provide a justification for considering that the activation energy for bulk and grain boundary diffusion are similar in this work. The experimental scatter and the scarcity of data provide a justification for considering that the activation energy for bulk and grain boundary diffusion are similar in this work. From those results it is thus possible to evaluate the diffusion ratio. Comparing the intra-granular and inter-granular experimental data reported in **Figure 4** it is possible to determine that the diffusion ratio varies in a range between $D_{gb}/D_{ig}{\sim}10^2$ and $D_{gb}/D_{ig}{\sim}10^4$. At the highest temperature at which data were collected (1373 K), the value of the ratio is $D_{gb}/D_{ig}{\sim}10^3$. Since this last value of the ratio is achieved at a temperature that is the closest (among the ones in **Figure 4**) to the holding temperature of the annealing history considered, it is assumed as the reference value for the diffusion ratio adopted in this work.

We can see from **Figure 3(b)** that the impact of the diffusion coefficient uncertainty on the fractional helium release is basically negligible for the temperature profile considered (and also for the other cases analysed in [10]). The impact of the diffusion coefficient is more significant on the helium release rate, since a smaller diffusion coefficient implies a first peak significantly delayed while a greater diffusion coefficient implies a first release rate peak occurring at lower temperature values.

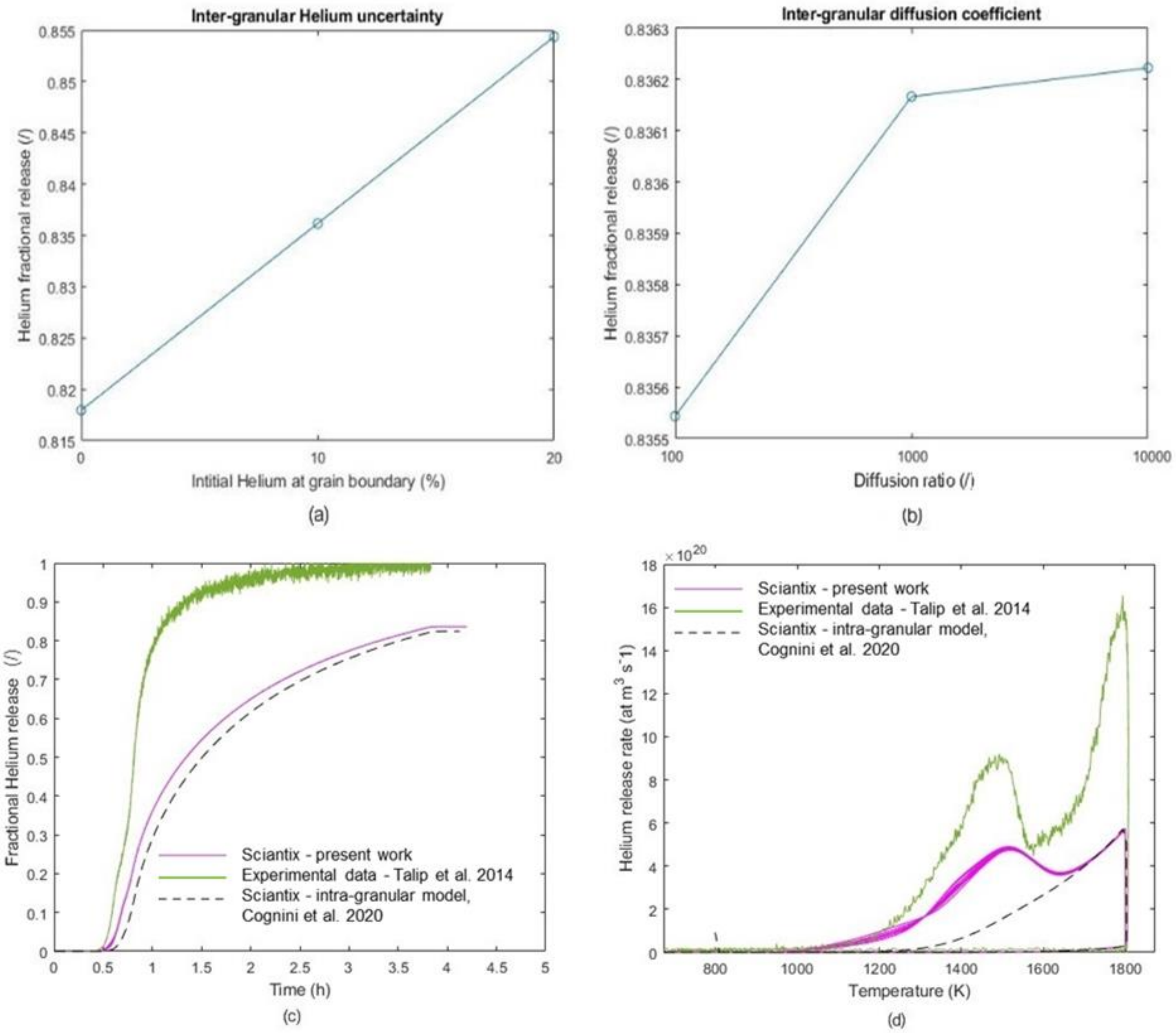

Figure 3: Effects of the uncertainty analysis on helium release behaviour: (a) effect of the fraction of helium initially present at grain boundaries on the fractional release, (b) effect of the diffusion coefficient on the fractional release, (c) bundle of curves that shows the effects on fractional release of how the fraction of helium initially present at grain boundaries is split between bubbles (in a range between 0% and 50%) and solution, (d) bundle of curves that shows the effects on release rate of how the fraction of helium initially present at grain boundaries is split between bubbles (in a range between 0% and 50%) and solution. The curves calculated with the reference model parameters are already reported in Figure 2 and correspond to the centre of the bundles in both plots (c) and (d).

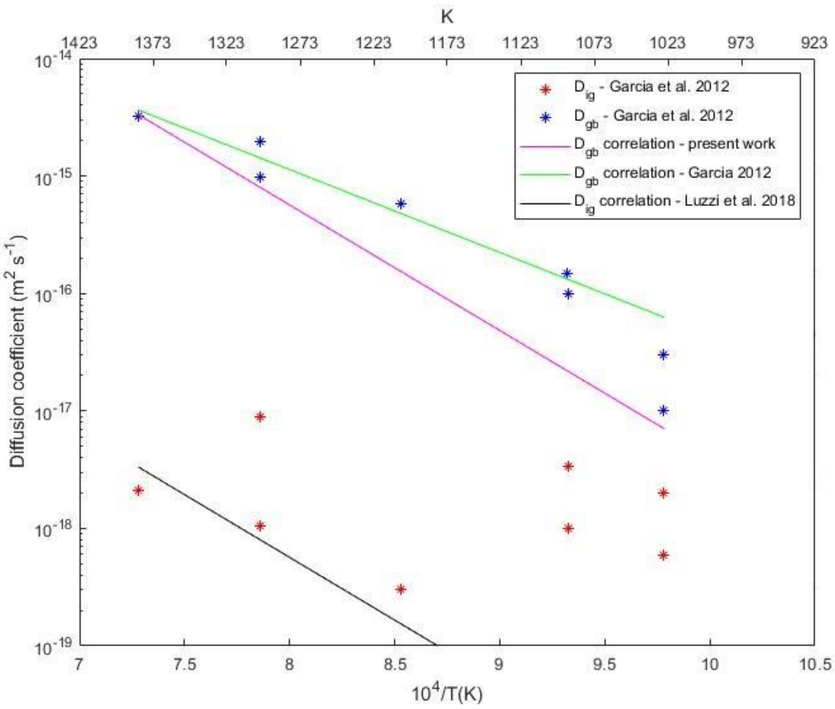

Figure 4: Helium diffusion coefficients within the grain (red data) and around the grain boundaries (blue data) [27]. Different correlation are reported on the graph: the correlation proposed for grain boundary diffusion in the samples studied by Garcia et al. (green line), the correlation adopted for grain boundary helium in this work (purple line) and the correlation adopted in the intra-granular helium model [10], [20].

5. Conclusion

In this work a new model for the description of helium evolution at grain boundaries is proposed. The model is implemented in SCIANTIX and aims at improving the predictive capabilities on helium behaviour by including a description of helium evolution at grain boundaries. The model is validated against a set of data collected during annealing experiments on UO_2 performed by Talip et al. (2014). The results show that the inclusion of a model treating helium behaviour at grain boundaries provides a promising overall improvement with respect to the version where the inter-granular contribution to helium evolution was not considered. This improvement can especially be appreciated on the release rate of the 1800 K history where the experimentally observed double peak, previously absent in the state-of-the-art predictions, becomes visible. The parametric analysis on some critical parameters showed that, within a reasonable range, they bear little impact on the final value of the release. Some of the features of the models can still be improved. First of all, a better description of the distribution factor and further investigation could identify the best approach to define this parameter. Then a more detailed experimental knowledge would allow to improve the quality of the assumptions made for the input parameters. Additional analyses could involve the identification of the "optimal" model parameters (in terms of initial fraction of helium at the grain boundary and inter-granular diffusion coefficient) providing the best agreement with the available experimental data on helium release and release rate. Lastly the definition of a proper diffusion coefficient rather than a simple diffusion ratio would allow accounting for a more precise evaluation of the diffusion at grain boundaries.

Acknowledgements

This work has received funding from the Euratom research and training programme 2019-2020 under grant agreement No 945077 (PATRICIA project).

References

[1] D. Pizzocri *et al.*, “A model describing intra-granular fission gas behaviour in oxide fuel for advanced engineering tools,” *J. Nucl. Mater.*, 2018, doi: 10.1016/j.jnucmat.2018.02.024.

[2] G. Pastore, L. Luzzi, V. Di Marcello, and P. Van Uffelen, “Physics-based modelling of fission gas swelling and release in UO 2 applied to integral fuel rod analysis,” *Nucl. Eng. Des.*, vol. 256, pp. 75–86, 2013, doi: 10.1016/j.nucengdes.2012.12.002.

[3] T. Barani *et al.*, “Analysis of transient fi ssion gas behaviour in oxide fuel using BISON and TRANSURANUS,” *J. Nucl. Mater.*, vol. 486, pp. 96–110, 2017, doi: 10.1016/j.jnucmat.2016.10.051.

[4] G. Pastore *et al.*, “Uncertainty and sensitivity analysis of fission gas behavior in engineering-scale fuel modeling,” *J. Nucl. Mater.*, vol. 456, pp. 398–408, 2015, doi: 10.1016/j.jnucmat.2014.09.077.

[5] T. Wiss *et al.*, “Properties of the high burnup structure in nuclear light water reactor fuel,” *Radiochim. Acta*, vol. 105, no. 11, pp. 893–906, 2017, doi: 10.1515/ract-2017-2831.

[6] D. Pizzocri, F. Cappia, L. Luzzi, G. Pastore, V. V Rondinella, and P. Van Uffelen, “A semi-empirical model for the formation and depletion of the high burnup structure in UO 2,” *J. Nucl. Mater.*, vol. 487, pp. 23–29, 2017, doi: 10.1016/j.jnucmat.2017.01.053.

[7] K. Lassmann, “TRANSURANUS: a fuel rod analysis code ready for use,” *Nucl. Mater. Fission React.*, pp. 295–302, 1992, doi: 10.1016/b978-0-444-89571-4.50046-3.

[8] B. Baurens, J. Sercombe, C. Riglet-martial, L. Desgranges, L. Trotignon, and P. Maugis, “3D thermo-chemical – mechanical simulation of power ramps with ALCYONE fuel code,” *J. Nucl. Mater.*, vol. 452, no. 1–3, pp. 578–594, 2014, doi: 10.1016/j.jnucmat.2014.06.021.

[9] W. Hales, J. D.; Williamson, R. L.; Novascone, S. R.; Pastore, G.; Spencer, B. W.; Stafford, D. S.; Gamble, K. A.; Perez, D. M.; Liu, “BISON Theory Manual The Equations behind Nuclear Fuel Analysis,” Idaho Falls, 2016. doi: https://doi.org/10.2172/1374503.

[10] L. Cognini, A. Cechet, T. Barani, D. Pizzocri, P. Van Uffelen, and L. Luzzi, “Towards a physics-based description of intra-granular helium behaviour in oxide fuel for application in fuel performance codes,” *Nucl. Eng. Technol.*, vol. 53, no. 2, pp. 562–571, 2021, doi: 10.1016/j.net.2020.07.009.

[11] H. J. Matzke, “Gas release mechanisms in UO2—a critical review,” *Radiat. Eff.*, vol. 53, no. 3–4, pp. 219–242, 1980, doi: 10.1080/00337578008207118.

[12] M. S. Veshchunov, “On the behaviour of intragranular ® ssion gas in UO 2 fuel,” *J. Nucl. Mater.*, vol. 277, pp. 67–81, 2000.

[13] D. R. Olander and D. Wongsawaeng, “Re-solution of fission gas - A review: Part I. Intragranular bubbles,” *J. Nucl. Mater.*, vol. 354, no. 1–3, pp. 94–109, 2006, doi: 10.1016/j.jnucmat.2006.03.010.

[14] M. Tonks *et al.*, “Unit mechanisms of fission gas release: Current understanding and future needs,” *J. Nucl. Mater.*, vol. 504, pp. 300–317, 2018, doi:

10.1016/j.jnucmat.2018.03.016.

[15] J. Rest, M. W. D. Cooper, J. Spino, J. A. Turnbull, P. Van Uffelen, and C. T. Walker, “Fission gas release from UO2 nuclear fuel: A review,” *J. Nucl. Mater.*, vol. 513, pp. 310–345, 2019, doi: 10.1016/j.jnucmat.2018.08.019.

[16] R. J. White, “The development of grain-face porosity in irradiated oxide fuel,” *J. Nucl. Mater.*, vol. 325, no. 1, pp. 61–77, 2004, doi: 10.1016/j.jnucmat.2003.10.008.

[17] D. Pizzocri, T. Barani, and L. Luzzi, “SCIANTIX: A new open source multi-scale code for fission gas behaviour modelling designed for nuclear fuel performance codes,” *J. Nucl. Mater.*, vol. 532, p. 152042, 2020, doi: 10.1016/j.jnucmat.2020.152042.

[18] L. Cognini *et al.*, “Helium solubility in oxide nuclear fuel: Derivation of new correlations for Henry’s constant,” *Nucl. Eng. Des.*, vol. 340, no. September, pp. 240–244, 2018, doi: 10.1016/j.nucengdes.2018.09.024.

[19] Z. Talip *et al.*, “Thermal diffusion of helium in 238Pu-doped UO2,” *J. Nucl. Mater.*, vol. 445, no. 1–3, pp. 117–127, 2014, doi: 10.1016/j.jnucmat.2013.10.066.

[20] L. Luzzi *et al.*, “Helium diffusivity in oxide nuclear fuel: Critical data analysis and new correlations,” *Nucl. Eng. Des.*, vol. 330, no. July 2017, pp. 265–271, 2018, doi: 10.1016/j.nucengdes.2018.01.044.

[21] D. R. Olander, “Fundamental Aspects of Nuclear Reactor Fuel Elements,” 1976.

[22] K. Nakajima, H. Serizawa, N. Shirasu, Y. Haga, and Y. Arai, “The solubility and diffusion coefficient of helium in uranium dioxide,” *J. Nucl. Mater.*, vol. 419, no. 1–3, pp. 272–280, 2011, doi: 10.1016/j.jnucmat.2011.08.045.

[23] F. Rufeh, D. R. Olander, and T. H. Pigford, “The Solubility of Helium in Uranium Dioxide,” *Nucl. Sci. Eng.*, vol. 23, no. 4, pp. 335–338, 1965, doi: 10.13182/nse65-a21069.

[24] E. Maugeri *et al.*, “Helium solubility and behaviour in uranium dioxide,” *J. Nucl. Mater.*, vol. 385, no. 2, pp. 461–466, 2009, doi: 10.1016/j.jnucmat.2008.12.033.

[25] R. M. DAVIES and S. G. TAYLOR, “The mechanics of large bubbles rising through extended liquids and through liquids in tubes,” *Dyn. Curved Front.*, vol. 200, no. 1062, pp. 377–392, 1988, doi: 10.1016/b978-0-08-092523-3.50041-1.

[26] J. Y. Colle *et al.*, “A mass spectrometry method for quantitative and kinetic analysis of gas release from nuclear materials and its application to helium desorption from UO 2 and fission gas release from irradiated fuel,” *J. Nucl. Sci. Technol.*, vol. 51, no. 5, pp. 700–711, 2014, doi: 10.1080/00223131.2014.889583.

[27] P. Garcia *et al.*, “A study of helium mobility in polycrystalline uranium dioxide,” *J. Nucl. Mater.*, vol. 430, no. 1–3, pp. 156–165, 2012, doi: 10.1016/j.jnucmat.2012.06.001.

[28] G. Martin *et al.*, “Helium release in uranium dioxide in relation to grain boundaries and free surfaces,” *Nucl. Instruments Methods Phys. Res. Sect. B Beam Interact. with Mater. Atoms*, vol. 268, no. 11–12, pp. 2133–2137, 2010, doi: 10.1016/j.nimb.2010.02.064.

[29] G. Martin *et al.*, “A quantitative µNRA study of helium intergranular and volume diffusion in sintered UO2,” *Nucl. Instruments Methods Phys. Res. Sect. B Beam Interact. with Mater. Atoms*, vol. 249, no. 1-2 SPEC. ISS., pp. 509–512, 2006, doi: 10.1016/j.nimb.2006.03.042.